Vortex lattice in anisotropic superconductors: The crossover from small B to large B

G. Preosti and Paul Muzikar
Department of Physics, Purdue University, West Lafayette, Indiana 47907
(Received 9 November 1992)

We discuss the tilted vortex lattice in layered type-II superconductors, using the anisotropic London theory. We pay particular attention to the crossover region between the low-B regime, in which vortex chain structure dominates, and the high-B region, where the chain structure has disappeared. This crossover region can be quite large, in some cases spanning several decades in magnetic field. We use both numerical calculation and simple physical arguments.

I. INTRODUCTION

The London theory of highly anisotropic type-II superconductors has recently been a subject of great interest[1-3] due to the investigation of the high-T_c oxide compounds.[4-6] The theory predicts that particular phenomena should arise when the magnetic field is not parallel to one of the crystalline axes. In that case, when $\gamma > 1$ [see Eq. (9)], at H_{c1} the magnetic field enters the superconductor in the form of chains of vortices; this contrasts with the situation in isotropic superconductors,[7] in which at H_{c1} single vortices begin to penetrate the material. At low flux densities the vortices form widely separated, weakly interacting chains; the chains constitute a highly distorted triangular lattice.

London theory can be used to compute how the lattice constants of the system vary with magnetic field. Daemen *et al.*,[8] in a pioneering paper, have investigated this problem. They find two simple regimes of behavior. At very low field the separation between two neighboring vortices in a chain, denoted by a, is essentially constant and independent of the magnetic field B. The distance between two chains, $L/2$ is a strong function of B, going as $1/B$. At very high field, quite different behavior results; both a and L vary as $1/\sqrt{B}$.

In this paper we discuss in some detail the crossover between the low-B and the high-B regime. One point we stress is that this crossover region can be quite large, spanning several decades in field. Over this range, the behavior of a and L is not particularly simple. In many ways the crossover region is the most interesting; the chainlike structure persists, yet the chains are close enough together to be strongly interacting. We use both numerical evaluations of the London free energy, and simple analytic approximations to develop our understanding of this system.

II. LONDON THEORY

We consider a vortex lattice of the form shown in Fig. 1. We describe it as a rectangular Bravais lattice in the xy plane with a two-point basis. The rectangular lattice is generated by the following two basis vectors:

$$\mathbf{a}_1 = a\hat{\mathbf{x}} , \tag{1}$$

$$\mathbf{a}_2 = L\hat{\mathbf{y}} . \tag{2}$$

Then $\mathbf{R} = n_1\mathbf{a}_1 + n_2\mathbf{a}_2$, where n_1 and n_2 are integers. Vortices parallel to the $\hat{\mathbf{z}}$ axis are located at the position $\mathbf{R} \pm \boldsymbol{\beta}$, where

$$\boldsymbol{\beta} = \frac{a}{4}\hat{\mathbf{x}} + \frac{L}{4}\hat{\mathbf{y}} . \tag{3}$$

The equation satisfied by the local magnetic field $\mathbf{h}(\mathbf{r})$ is

$$h_i + \lambda^2 \varepsilon_{ijk}\varepsilon_{ast} M_{ka}\partial_j\partial_s h_t = \hat{z}_i \Phi_0 \sum_{\{\mathbf{R}\}} [\delta^{(2)}(\mathbf{r}-\mathbf{R}-\boldsymbol{\beta}) + \delta^{(2)}(\mathbf{r}-\mathbf{R}+\boldsymbol{\beta})] . \tag{4}$$

Here we follow the notation of Daemen *et al.*[8] λ is the average penetration depth, Φ_0 is the superconducting flux quantum $hc/2e$, and M_{ij} is the dimensionless effective-mass tensor, normalized so that $\det(M) = 1$. The anisotropy axis of the crystal is $\hat{c}$, so we have

$$M_{ij} = M_c\hat{c}_i\hat{c}_j + M_a(\hat{a}_i\hat{a}_j + \hat{b}_i\hat{b}_j) , \tag{5}$$

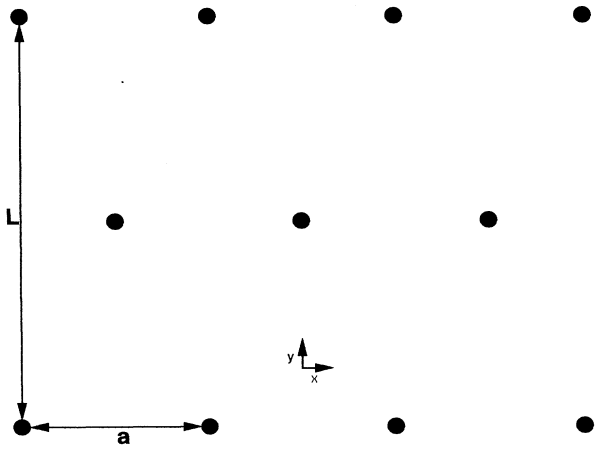

FIG. 1. Geometry of the vortex lattice. The distance between chains is $L/2$, and the separation between neighboring vortices within a chain is a.

with $M_c M_a^2=1$. The vortex axis z is rotated by θ with respect to the anisotropy axis c. Thus

$$\hat{\mathbf{z}}=\hat{\mathbf{c}}\cos\theta+\hat{\mathbf{a}}\sin\theta\ , \tag{6}$$

$$\hat{\mathbf{x}}=-\hat{\mathbf{c}}\sin\theta+\hat{\mathbf{a}}\cos\theta\ , \tag{7}$$

$$\hat{\mathbf{y}}=\hat{\mathbf{b}}\ . \tag{8}$$

the anisotropy parameter γ is defined by

$$\gamma=(M_c/M_a)^{1/2}\ . \tag{9}$$

The reciprocal-lattice vectors $\{\mathbf{G}\}$ are given by

$$\mathbf{G}=n_1\frac{2\pi}{a}\hat{\mathbf{x}}+n_2\frac{2\pi}{L}\hat{\mathbf{y}}\ , \tag{10}$$

where n_1 and n_2 are integers.

The London free energy per unit volume is given by[2]

$$F(a,L)=\frac{\Phi_0^2}{2\pi a^2L^2}\sum_{\{\mathbf{G}\}}\phi(\mathbf{G})\frac{[1+\lambda_1^2G^2(1+\varepsilon\cos^2\theta)]\cos^2(\mathbf{G}\cdot\boldsymbol{\beta})}{(1+\lambda_1^2G^2)[1+\lambda_1^2G_y^2(1+\varepsilon)+\lambda_1^2G_x^2(1+\varepsilon\cos^2\theta)]}\ , \tag{11}$$

where we have defined a new length scale λ_1 by

$$\lambda_1=\lambda\gamma^{-1/3} \tag{12}$$

and a parameter ε by

$$\varepsilon=\gamma^2-1\ . \tag{13}$$

The function $\phi(\mathbf{G})$ is a cutoff function, which is equal to unity at small values of $|\mathbf{G}|$, and goes to zero at large values of $|\mathbf{G}|$. This is a necessary evil, since otherwise the sum over $\{\mathbf{G}\}$ diverges at large $|\mathbf{G}|$; this simply reflects the failure of the London theory at short length scales. For our calculation we have followed the suggestion of Brandt,[9] and employed an anisotropic Gaussian

$$\phi(\mathbf{G})=\exp[-\alpha(G_x^2\xi_x^2+G_y^2\xi_y^2)]\ . \tag{14}$$

Here α is a numerical parameter and the coherence lengths ξ_x and ξ_y are defined by

$$\frac{\xi_x^2}{\xi_y^2}=\cos^2\theta+\frac{1}{\gamma^2}\sin^2\theta \tag{15}$$

and

$$\xi_y^2=\gamma^{2/3}\frac{\lambda^2}{\kappa^2}\ . \tag{16}$$

Here κ, defined by Daemen *et al.*,[8] is an averaged Ginzburg-Landau parameter, which we expect to be much larger than unity for the extremely type-II high-T_c materials. We will usually follow Daemen *et al.*[8] and take $\kappa=60$. The magnetic field $\mathbf{h}(\mathbf{r})$ generated by (4) has nonzero components in the x, y, and z directions. However, the average over a unit cell of $h_x(\mathbf{r})$ and $h_y(\mathbf{r})$ vanishes, and we define B as

$$B=\frac{1}{aL}\int_{\text{cell}}d^2r\,h_z(\mathbf{r})\ . \tag{17}$$

It is easy to check that

$$B=\frac{2\Phi_0}{aL}\ . \tag{18}$$

For a fixed B, we must then find the choice of a and L that minimizes F, subject to the product aL being fixed.

III. RESULTS

In Fig. 2 we show computed values of a/λ, as a function of magnetic field, for three angles of $\theta=80°$, 70°, and 60°. We follow Daemen *et al.*[8] in choosing $\gamma=55$ and $\kappa=60$; many of the high-T_c oxide compounds, such as $Bi_2Sr_2CaCu_2O_8$, are indeed highly anisotropic.

As expected a/λ is constant at small B, and assumes a $1/\sqrt{B}$ behavior at large B. The broad crossover region is clearly seen. For example, for $\theta=60°$, it extends from $B\approx 0.016\Phi_0/\lambda^2$ to $B\approx 2.5\Phi_0/\lambda^2$. In Fig. 3 we show results for $\theta=30°$, 40°, and 50°. Again the crossover region is quite broad.

We can make simple theoretical estimates to understand the origin of the crossover region. We discuss the small-B limit first. For small B we can approximate F by the following formula:

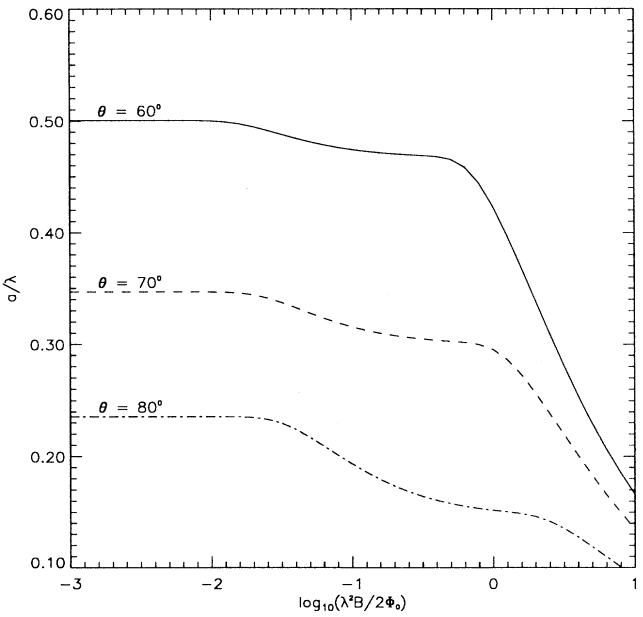

FIG. 2. a/λ as a function of B, for three different angles. In this calculation we took $\kappa=60$ and $\gamma=55$; the cutoff parameter was set at $\alpha=0.02$.

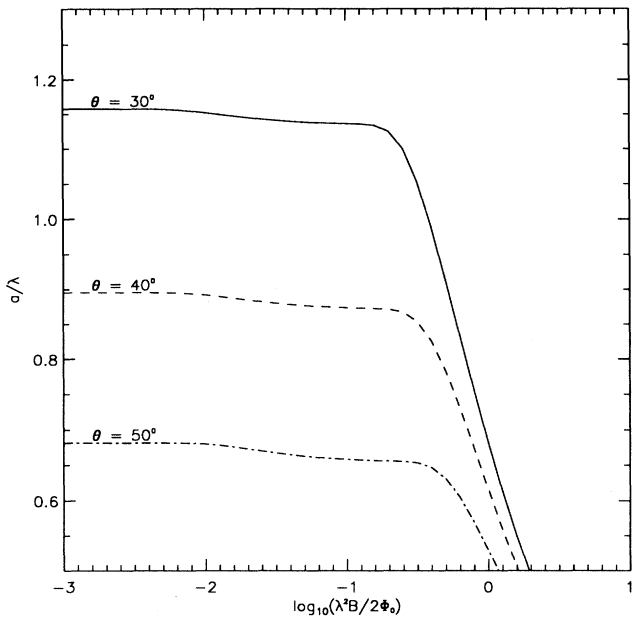

FIG. 3. a/λ as a function of B, for three different angles. As in Fig. 2, we have $\kappa=60$, $\gamma=55$, and $\alpha=0.02$.

$$F(a,L)=\frac{\Phi_0^2}{8\pi aL}\left[c_0\left[\frac{a-a_0}{a_0}\right]^2+\frac{2\sin^2\theta}{a\lambda_1\sqrt{1+\varepsilon}}\times\exp\left[-\frac{L}{2\lambda_1\sqrt{1+\varepsilon}}\right]\right]. \quad (19)$$

The energy of a single isolated chain has a minimum at

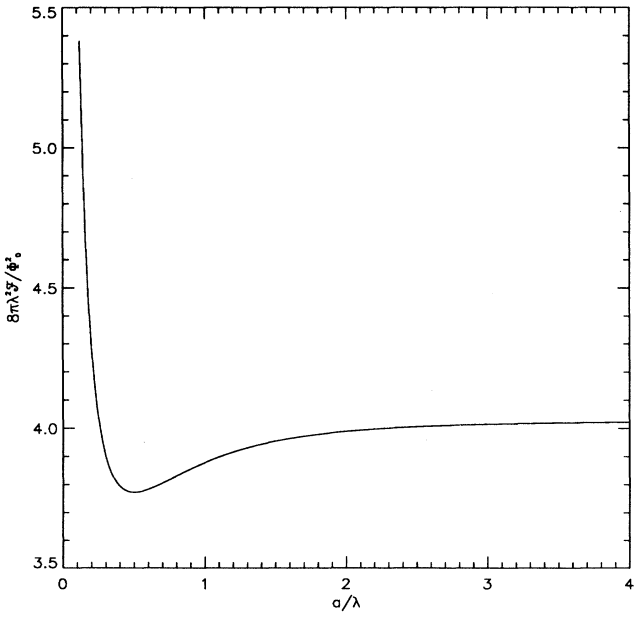

FIG. 4. Free energy per vortex per unit length (in $\hat{z}$) of an isolated vortex chain, as a function of a/λ. For the calculation we chose $\kappa=60$, $\gamma=55$, $\alpha=0.02$, and $\theta=60°$.

TABLE I. Coefficients c_0 and a_0 for $\gamma=55$, $\kappa=60$, and $\alpha=0.02$.

θ	a_0/λ	$c_0\lambda^2$
10°	2.05	8.67×10^{-3}
20°	1.50	7.09×10^{-2}
30°	1.16	2.63×10^{-1}
40°	0.895	6.96×10^{-1}
50°	0.682	1.52
60°	0.500	2.95
70°	0.347	5.17
80°	0.236	6.38

$a=a_0$; for small deviations from a_0 we write the energy per unit length per vortex of a single isolated chain as

$$\mathcal{F}=\frac{\Phi_0^2}{8\pi}\frac{c_0}{2}\left[\frac{a-a_0}{a_0}\right]^2. \quad (20)$$

This is the origin of the first term in (19). The coefficient c_0 is determined numerically from computations of the single chain energy as a function of a, as is the value of a_0. Tables I–III show the numerical values for both c_0 and a_0, while Fig. 4 shows a plot of the energy per unit length per vortex as a function of a, for a particular choice of parameters.

The second term in (19) represents the interaction between chains when L is very large. This asymptotic formula is determined by Buzdin and Simonov.[2]

If we use (18), we can rewrite (19) as

$$F=\frac{1}{2}\frac{\Phi_0 B}{8\pi}\left[c_0\left[\frac{a-a_0}{a_0}\right]^2+\frac{2\sin^2\theta}{a\lambda_1\sqrt{1+\varepsilon}}\times\exp\left[-\frac{\Phi_0}{\lambda_1 aB\sqrt{1+\varepsilon}}\right]\right]. \quad (21)$$

So, we must minimize F with respect to a at fixed B; this should give reasonable answers for small B.

We can also make an estimate relevant to the high-B end of the crossover region. The $1/\sqrt{B}$ behavior in a and L results from Eq. (11) when we are in the limit $G^2\lambda_1^2\gg1$ for all $\mathbf{G}$ except $\mathbf{G}=\mathbf{0}$[1]:

TABLE II. Coefficients c_0 and a_0 for $\gamma=25$, $\kappa=60$, and $\alpha=0.02$.

θ	a_0/λ	$c_0\lambda^2$
10°	2.71	2.62×10^{-3}
20°	2.00	2.17×10^{-2}
30°	1.54	8.05×10^{-2}
40°	1.20	2.10×10^{-1}
50°	0.931	4.48×10^{-1}
60°	0.705	8.15×10^{-1}
70°	0.527	1.21
80°	0.454	8.96×10^{-1}

TABLE III. Coefficients c_0 and a_0 for $\gamma=5$, $\kappa=60$, and $\alpha=0.02$.

θ	a_0/λ	$c_0\lambda^2$
10°	5.34	7.75×10^{-5}
20°	4.02	7.51×10^{-4}
30°	3.23	2.84×10^{-3}
40°	2.67	6.84×10^{-3}
50°	2.28	1.18×10^{-2}
60°	2.06	1.39×10^{-2}
70°	2.13	7.92×10^{-3}
80°	3.46	2.55×10^{-4}

$$F\approx\frac{\Phi_0^2}{2\pi a^2L^2}+\frac{\Phi_0^2(1+\varepsilon\cos^2\theta)}{2\pi a^2L^2}\times\sum_{\{\mathbf{G}\neq0\}}\frac{\cos^2(\mathbf{G}\cdot\boldsymbol{\beta})}{(1+\varepsilon)G_y^2+(1+\varepsilon\cos^2\theta)G_x^2}\ . \tag{22}$$

We can then ask, if we start at a very high B and then lower B so that a and L increase, when does the approximation (22) begin to break down? Since $L>a$ and $\varepsilon>0$, this condition is

$$\frac{2\pi}{L}\approx\frac{1}{\lambda_1}\ . \tag{23}$$

As shown previously[1,2] in the high-B limit we have

$$\frac{L}{a}=\left[\frac{3(1+\varepsilon)}{1+\varepsilon\cos^2\theta}\right]^{1/2}\ . \tag{24}$$

Thus, when (23) holds we have

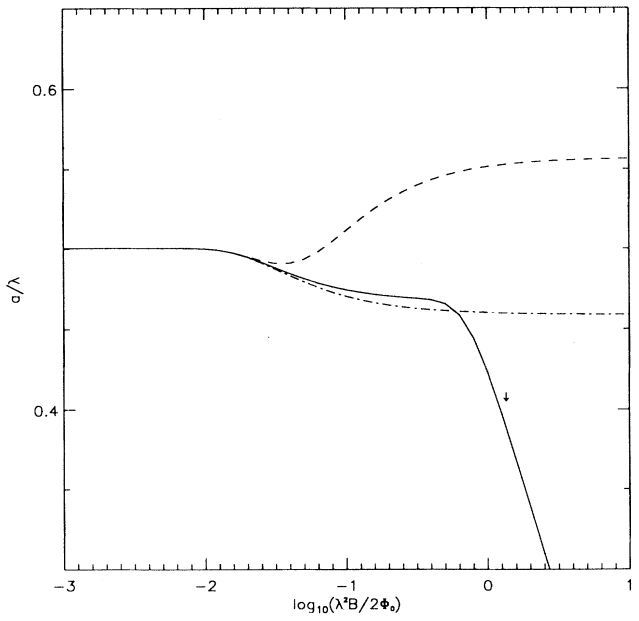

FIG. 5. Comparison of several simple approximations with the true London theory result (solid line). We have chosen $\kappa=60$, $\gamma=55$, $\alpha=0.02$, and $\theta=60°$. The dashed line comes from Eq. (19) and the dash-dot line from Eq. (A5). The arrow marks the B field predicted by Eq. (26).

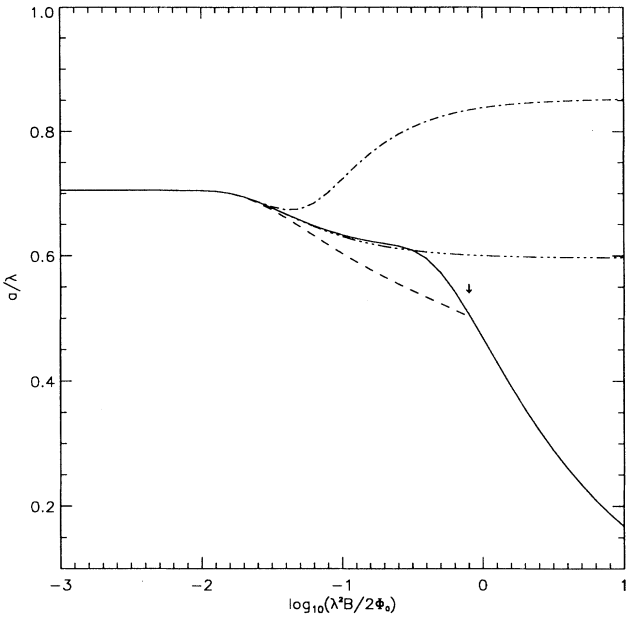

FIG. 6. Comparison of several simple approximations with the true London theory results (solid line) for $\kappa=60$, $\gamma=25$, $\alpha=0.02$, and $\theta=60°$. The dashed line comes from Eq. (A5), the dash-dot line from Eq. (19), and the dash-three-dot line comes from Eq. (A5) with a cubic term added to the intrachain energy. The arrow marks the B field predicted by Eq. (26).

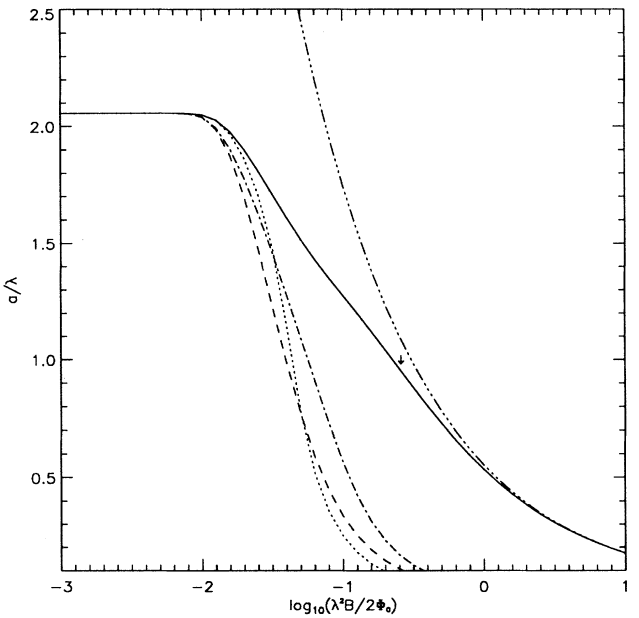

FIG. 7. Comparison of several simple approximations with the true London theory result (solid line), for $\kappa=60$, $\gamma=5$, $\alpha=0.02$, and $\theta=60°$. The dotted line comes from Eq. (19), the dashed line from Eq. (A5), and the dashed-dot line from Eq. (A5) with a cubic term added to the intrachain energy. The dashed-three-dot line is the prediction of the high-B theory [Eq. (24)], while the arrow marks the B field predicted by Eq. (26).

$$aL \approx 4\pi^2\lambda_1^2 \left[\frac{1+\varepsilon\cos^2\theta}{3(1+\varepsilon)} \right]^{1/2} . \tag{25}$$

this predicts that the high-field limit of the crossover region is given by

$$B \approx \frac{\Phi_0}{2\pi^2\lambda_1^2} \left[\frac{3(1+\varepsilon)}{1+\varepsilon\cos^2\theta} \right]^{1/2} . \tag{26}$$

In Fig. 5 we compare the prediction obtained from Eq. (21) to the results obtained from minimizing the full free energy [Eq. (11)]. We see that the quite simple approximation embodied in (21) predicts nicely the initial downturn in a/λ as B increases but for large B it goes wrong badly. We also show in Fig. 5 the results of minimizing an improved approximate formula. The improved approximation is discussed in the Appendix. Finally, the arrow in Fig. 5 denotes the prediction of Eq. (26); for B larger than this, a and L should both scale as $1/\sqrt{B}$.

In Figs. 6 and 7 we show results for $\gamma=25$ and $\gamma=5$; in both cases we chose $\theta=60°$. We note that the approximations (21) and (31) fail sooner as B increases into the crossover regime, particularly for $\gamma=5$. As discussed in the Appendix, one of the reasons for this is that as γ gets smaller, the parabolic approximation for the intrachain energy [Eq. (20)] becomes less satisfactory. Thus in these two figures we also show the result of adding a cubic term to the intrachain energy. The coefficient of the cubic term was determined from the numerically computed single chain energy.

ACKNOWLEDGMENTS

We thank Luc Daemen for providing us with early versions of his results. We are grateful to him and to Mario Palumbo for useful conversations. This work was supported by the National Science Foundation under Grant No. DMR88-09854 through the Science and Technology Center for Superconductivity.

APPENDIX

In this Appendix we discuss in more detail the derivation of approximate free-energy formulas. The starting point is Eq. (11) for $F(a,L)$; we follow the path described by Buzdin and Simonov.[2] In Eq. (11) we perform the sum on G_y using the Poisson summation formula. To do this, we set the cutoff function, $\phi(\mathbf{G})$, equal to 1. This yields the following result:

$$F(a,L)=F^{(1)}(a,L)+F^{(2)}(a,L) , \tag{A1}$$

$$F^{(1)}(a,L)=\frac{\Phi_0^2}{8\pi a^2 L}\sum_{\{G_x\}}\left[\frac{\sin^2\theta}{\lambda_1\sqrt{1+\varepsilon}} \frac{\sqrt{1+\lambda_1^2G_x^2(1+\varepsilon\cos^2\theta)}}{1+\lambda_1^2G_x^2\sin^2\theta} + \frac{\cos^2\theta}{\lambda_1} \frac{1}{(1+\lambda_1^2G_x^2\sin^2\theta)\sqrt{1+\lambda_1^2G_x^2}} \right] , \tag{A2}$$

$$F^{(2)}(a,L)=\frac{\Phi_0^2}{4\pi a^2 L}\sum_{\{G_x\}}\left[\frac{\sin^2\theta}{\lambda_1\sqrt{1+\varepsilon}} \frac{\sqrt{1+\lambda_1^2G_x^2(1+\varepsilon\cos^2\theta)}}{1+\lambda_1^2G_x^2\sin^2\theta} \frac{\pm 1}{\exp[(L/(2\lambda_1\sqrt{1+\varepsilon}))\sqrt{1+\lambda_1^2G_x^2(1+\varepsilon\cos^2\theta)}]\mp 1} + \frac{\cos^2\theta}{\lambda_1} \frac{1}{(1+\lambda_1^2G_x^2\sin^2\theta)\sqrt{1+\lambda_1^2G_x^2}} \frac{\pm 1}{\exp[(L/2\lambda_1)\sqrt{1+\lambda_1^2G_x^2}]\mp 1} \right] . \tag{A3}$$

In the sum, the upper sign has to be used for even or zero m and the lower sign for odd m, where $G_x=2\pi m/a$.

Here, $F^{(1)}(a,L)$ represents the energy density of a set of independent chains, and $F^{(2)}(a,L)$ is caused by the interaction energy between the chains.

The sum in (A2) diverges and needs a cutoff; this simply replaces the cutoff function $\phi(\mathbf{G})$ used in Eq. (11) with a different cutoff procedure. We are interested in (A3), the chain-chain interaction term. Our goal is to evaluate the dominant, large-L behavior of (A3). We first note that the $G_x=0$ term is most important at large L. Next, we note that if $\sqrt{1+\varepsilon}\gg 1$, the first term in brackets in (A3) dominates the second. We are thus led to the following approximation formula:

$$F^{(2)}(a,L)\approx\frac{\Phi_0^2}{8\pi a^2 L}\frac{2\sin^2\theta}{\lambda_1\sqrt{1+\varepsilon}}\frac{1}{\exp(L/(2\lambda_1\sqrt{1+\varepsilon}))-1} . \tag{A4}$$

Combining this with Eq. (20), we arrive at the following approximation for $F(a,L)$:

$$F(a,L)\approx\frac{1}{2}\frac{\Phi_0 B}{8\pi}\left[c_0\left[\frac{a-a_0}{a_0}\right]^2 + \frac{2\sin^2\theta}{a\lambda_1\sqrt{1+\varepsilon}}\frac{1}{\exp(L/(2\lambda_1\sqrt{1+\varepsilon}))-1} \right] . \tag{A5}$$

We stress that this approximation is best for highly anisotropic superconductors, which have $\varepsilon\gg 1$. The smaller the value of ε, the more quickly neglected terms become important as L decreases. Another important effect is that as ε gets smaller, the parabolic approximation of Eq. (20) breaks down more quickly as B enters the crossover region. When c_0 is too small, the parabola is not stiff enough to prevent a from assuming unrealistically small values.

[1]L. J. Campbell, M. M. Doria, and V. G. Kogan, Phys. Rev. B **38**, 2439 (1988).
[2]A. I. Buzdin and A. Yu. Simonov, Physica C **175**, 143 (1991).
[3]A. M. Grishin, A. Yu. Martynovich, and S. V. Yampol'skii, Zh. Teor. Fiz. **97**, 1930 (1990) [Sov. Phys. JETP **70**, 1089 (1990)].
[4]C. A. Bolle, P. L. Gammel, D. G. Grier, C. A. Murray, D. J. Bishop, D. B. Mitzi, and A. Kapitulnik, Phys. Rev. Lett. **66**, 112 (1991).
[5]P. L. Gammel, D. J. Bishop, J. P. Rice, and D. M. Ginsberg, Phys. Rev. Lett. **68**, 3343 (1992).
[6]G. J. Dolan, F. Holtzberg, C. Field, and T. R. Dinger, Phys. Rev. Lett. **62**, 2184 (1989).
[7]M. Tinkham, *Introducton to Superconductivity* (McGraw-Hill, New York, 1975), p. 144.
[8]L. L. Daemen, L. J. Campbell, and V.G. Kogan, Phys. Rev. B **46**, 3631 (1992).
[9]E. H. Brandt, Physica C **195**, 1 (1992).